Application of block diagonal technique to Hamiltonian matrix in performing spin-splitting calculations for GaAs zincblende bulk and quantum wells

目 錄：

(一)計畫成果自評，(二)報告內容與參考文獻

(一) 計畫成果自評：

已完成半導體自旋分裂(spin-splitting)之探討，並被 American Institute of Physics 協會收錄於 Journal of Applied Physics 期刊(Impact Factor: 2.137)。

與國科會計劃 90%相符。

(二) 報告內容與參考文獻：

看以下 9 頁論文：Chun-Nan Chen(1st author) et. al. J. Appl. Phys. 104 (2008) 024901-1~024901-9.

Application of block diagonal technique to Hamiltonian matrix in performing spin-splitting calculations for GaAs zincblende bulk and quantum wells

Chun-Nan Chen,[1,a)] Wei-Long Su,[2] Kuo-Ching Chang,[3,b)] Sheng-Hsiung Chang,[3] Jih-Chen Chiang,[4,c)] Ikai Lo,[4] Wan-Tsang Wang,[4] Hsiu-Fen Kao,[4] and Meng-En Lee[4]
[1]*Quantum Science Simulation and Computing Laboratory, Department of Physics, Tamkang University, 151 Ying-chuan Road, Tamsui, Taipei County, Taiwan 25137, People's Republic of China*
[2]*Department of Electronic Engineering, Lee-Ming Institute of Technology, Taishan, Taipei County, Taiwan 24305, People's Republic of China*
[3]*Department of Electronic Engineering, Far-East University, Hsin-Shih Town, Tainan County, Taiwan 744, People's Republic of China*
[4]*Department of Physics, National Sun Yat-Sen University, Kaohsiung 80424, Taiwan, People's Republic of China*

(Received 14 December 2007; accepted 14 February 2008; published online 17 July 2008)

The 2×2 conduction band, 4×4 hole band, and 2×2 spin-orbit split-off band matrices of zincblende semiconductors are obtained by using a block diagonal technique. Importantly, the block diagonal matrices incorporate not only the interband coupling effect but also the bulk inversion asymmetry effect. Analytical expressions for the conduction band spin-splitting energies of GaAs zincblende bulk and quantum wells grown on [001]-, [111]-, and [110]-oriented substrates are formulated by solving the block diagonal matrices. The results show that odd-in-k terms exist in both the bulk and the quantum well expressions due to the bulk inversion asymmetry effect. The presence of these terms is shown to induce the spin-splitting phenomenon. © *2008 American Institute of Physics*. [DOI: 10.1063/1.2907445]

I. INTRODUCTION

The fine details of the electronic structures of semiconductors and their heterostructures are well understood. However, an increasing interest in the hyperfine details of these structures, such as their spin-splitting characteristics, for instance, has led to the emergence of a new research field known as spintronics.[1–5] The electron states in a crystal are known to be doubly degenerate if the system has both time reversal and space inversion symmetries. However, the spin degeneracy property is lost under the application of an external magnetic field since the time reversal symmetry is destroyed.[6] Furthermore, the lack of inversion symmetry due to the crystalline structure itself or due to the application of an external force field (e.g., strain, electric field, and structural confinement) may also result in the loss of spin degeneracy.[7,8]

The loss of spin degeneracy in semiconductor heterostructures in the zero-field condition has attracted considerable attention in the spintronics field. It is believed that zero-field spin splitting may be induced by one of two different mechanisms, namely, (i) a k^3 term in the conduction and valence band expressions related to microscopic inversion asymmetry (generally referred to as the Dresselhaus effect) or (ii) an interfacial spin-orbit interaction term (referred to as the Rashba effect).[9,10] The purpose this study is to analyze the k^3 term to formulate its analytical mathematical forms for zincblende bulk and quantum wells (QWs) oriented along different growth directions, respectively.

Zincblende semiconductors exhibit an intrinsic spin-splitting effect as a result of the inversion asymmetry of their microscopic crystal potential. Consequently, the valence band structure may include a linear-in-k term, which is associated with the Kane C parameter.[11] However, calculations by Cardona *et al.*[12] showed that the resulting splitting effect is extremely small. In addition, a cubic-in-k (k^3) term, which is associated with the Kane B parameter (denoted as B_0 in this paper) and potentially is of significant magnitude, may appear in both the conduction band and the valence band structures.[11] Splitting effects have also been observed in spin-polarized photoemission and infrared spin resonance.[13,14] By neglecting the linear-in-k (C parameter) term, i.e., by considering only the cubic-in-k (B parameter) term, this paper derives analytical expressions for the spin-splitting effect as a function of the components of the wave vector $\mathbf{k}$ in GaAs zincblende bulk and GaAs QWs grown on [001]-, [111]- and [110]-oriented substrates.

In the adopted approach, the rotation technique is applied to the 8×8 $\boldsymbol{k}\cdot\boldsymbol{p}$ Hamiltonian matrix of bulk zincblende semiconductors.[15,16] The conduction band and valence bands are then decoupled by applying the block diagonal technique to the rotated 8×8 Hamiltonian matrix.[17] The resulting 2×2 conduction Hamiltonian matrix along arbitrary k directions is then solved to obtain analytical expressions for the spin splitting of the conduction band.

[a)]Electronic mail: quantum@mail.tku.edu.tw.
[b)]Electronic mail: cauchy_chang@yahoo.com.tw.
[c)]Electronic mail: chiang@mail.phys.nsysu.edu.tw.

II. THEORETICAL METHODS

In semiconductor physics, the conventional $\boldsymbol{k}\cdot\boldsymbol{p}$ formalism does not take into account the tetrahedral symmetry within a unit cell. However, this symmetry property can be accounted for by inserting the Kane B parameter terms (i.e., $B_0k_xk_y$, $B_0k_yk_z$, and $B_0k_xk_z$) into the $\boldsymbol{k}\cdot\boldsymbol{p}$ Hamiltonian matrix.[11] The resulting [001]-oriented $\boldsymbol{k}\cdot\boldsymbol{p}$ Hamiltonian (in the sp^3 basis ordering as $|S\rangle$, $|X\rangle$, $|Y\rangle$, $|Z\rangle$) has the form[11]

$$H=\begin{bmatrix} E_c+\hbar^2k^2/2m_c & B_0(\vec{q}\cdot\hat{x})+iP_0(\vec{k}\cdot\hat{x}) & B_0(\vec{q}\cdot\hat{y})+iP_0(\vec{k}\cdot\hat{y}) & B_0(\vec{q}\cdot\hat{z})+iP_0(\vec{k}\cdot\hat{z}) \\ B_0(\vec{q}\cdot\hat{x})-iP_0(\vec{k}\cdot\hat{x}) & E_v+Lk_x^2+M(k_y^2+k_z^2) & Nk_xk_y & Nk_xk_z \\ B_0(\vec{q}\cdot\hat{y})-iP_0(\vec{k}\cdot\hat{y}) & Nk_xk_y & E_v+Lk_y^2+M(k_z^2+k_x^2) & Nk_yk_z \\ B_0(\vec{q}\cdot\hat{z})-iP_0(\vec{k}\cdot\hat{z}) & Nk_xk_z & Nk_yk_z & E_v+Lk_z^2+M(k_x^2+k_y^2) \end{bmatrix}, \tag{1}$$

where $\vec{k}=k_x\hat{x}+k_y\hat{y}+k_z\hat{z}$, $\vec{q}=k_yk_z\hat{x}+k_zk_x\hat{y}+k_xk_y\hat{z}$, P_0 (in units of eV Å) is the Kane parameter, i.e., $P_0=\hbar/m_0\langle s|p_x|x\rangle$, and B_0 (in units of eV Å^2) is given by

$$B_0=2\frac{\hbar^2}{m^2}\sum_j^{\Gamma_{15}}\frac{\langle s|p_x|u_j\rangle\langle u_j|p_y|z\rangle}{[(E_c+E_v)/2-E_j]}.$$

It is noted that in Eq. (1), the B_0 terms are the only matrix elements that are incompatible with inversion symmetry.

The Hamiltonian for arbitrary orientations can be obtained by rotating the [001]-oriented Hamiltonian from the (x,y,z) lattice coordinate system to an arbitrarily oriented (x',y',z') coordinate system.[15,16] The following rotation matrix can be used to derive the basis functions in the general coordinate system:

$$O_T=\begin{bmatrix} O_{11} & O_{12} & O_{13} \\ O_{21} & O_{22} & O_{23} \\ O_{31} & O_{32} & O_{33} \end{bmatrix}. \tag{2}$$

If the rotation from $z=[001]$ to z' is governed by the orthogonal transformation $r'=O_Tr$, then the same rotation must also be applied to both the wave vector ($\mathbf{k}$) and the linear combination coefficients of the basis.[15,16]

The Hamiltonian for arbitrary orientations $[hkl]$ (in the spin-orbit coupling basis ordering as $|iS\uparrow'\rangle$, $|iS\downarrow'\rangle$, $|3/2,3/2\rangle'$, $|3/2,1/2\rangle'$, $|3/2,-1/2\rangle'$, $|3/2,-3/2\rangle'$, $|1/2,1/2\rangle'$, $|1/2,-1/2\rangle'$) can be expressed as[15,16]

$$H_{8\times8}^{[hkl]}(\mathbf{k})=\begin{bmatrix} A' & 0 & S & T & \frac{R}{\sqrt{3}} & 0 & \frac{T}{\sqrt{2}} & \frac{\sqrt{2}}{\sqrt{3}}R \\ 0 & A' & 0 & \frac{S}{\sqrt{3}} & T & R & -\frac{\sqrt{2}}{\sqrt{3}}S & -\frac{T}{\sqrt{2}} \\ S^* & 0 & P+Q & D & C & 0 & \frac{D}{\sqrt{2}} & \sqrt{2}C \\ T^* & \frac{S^*}{\sqrt{3}} & D^* & P-Q & 0 & C & -\sqrt{2}Q & -\frac{\sqrt{3}}{\sqrt{2}}D \\ \frac{R^*}{\sqrt{3}} & T^* & C^* & 0 & P-Q & -D & -\frac{\sqrt{3}}{\sqrt{2}}D^* & \sqrt{2}Q \\ 0 & R^* & 0 & C^* & -D^* & P+Q & -\sqrt{2}C^* & \frac{D^*}{\sqrt{2}} \\ \frac{T^*}{\sqrt{2}} & -\frac{\sqrt{2}}{\sqrt{3}}S^* & \frac{D^*}{\sqrt{2}} & -\sqrt{2}Q & -\frac{\sqrt{3}}{\sqrt{2}}D & -\sqrt{2}C & P-\Delta & 0 \\ \frac{\sqrt{2}}{\sqrt{3}}R^* & -\frac{T^*}{\sqrt{2}} & \sqrt{2}C^* & -\frac{\sqrt{3}}{\sqrt{2}}D^* & \sqrt{2}Q & \frac{D}{\sqrt{2}} & 0 & P-\Delta \end{bmatrix}, \tag{3}$$

where * denotes the Hermitian conjugate, and the matrix elements can be written as

$$A' = E_c + \frac{\hbar^2 k^2}{2m_c},$$

$$S = -\tfrac{1}{\sqrt{2}}\langle iS|H|X' + iY'\rangle,$$

$$R = \tfrac{1}{\sqrt{2}}\langle iS|H|X' - iY'\rangle,$$

$$T = \tfrac{\sqrt{2}}{\sqrt{3}}\langle iS|H|Z'\rangle,$$

$$C = -\tfrac{1}{2\sqrt{3}}\langle X' + iY'|H|X' - iY'\rangle,$$

$$D = -\tfrac{1}{\sqrt{3}}\langle X' + iY'|H|Z'\rangle,$$

$$P = \tfrac{1}{3}\langle X' + iY'|H|X' + iY'\rangle + \tfrac{1}{3}\langle Z'|H|Z'\rangle,$$

and

$$Q = \tfrac{1}{6}\langle X' + iY'|H|X' + iY'\rangle - \tfrac{1}{3}\langle Z'|H|Z'\rangle.$$

The 8×8 Hamiltonian matrix in Eq. (3) can be block diagonalized such that the conduction band and the valence bands are decoupled.[17] The resulting 2×2 conduction Hamiltonian matrix in the $[hkl]$ orientation can then be written as

$$H_{2\times 2}^{(c)} = \begin{bmatrix} A_c & \Omega_c \\ \Omega_c^* & B_c \end{bmatrix} = \begin{bmatrix} \frac{A_c + B_c}{2} & 0 \\ 0 & \frac{A_c + B_c}{2} \end{bmatrix} + \begin{bmatrix} \frac{A_c - B_c}{2} & \Omega_c \\ \Omega_c^* & -\frac{A_c - B_c}{2} \end{bmatrix}, \tag{4}$$

where

$$A_c = A' + (SS^* + TT^* + RR^*/3)\left(\frac{1}{E_g}\right) + (TT^*/2 + 2RR^*/3)\times\left(\frac{1}{E_g + \Delta}\right),$$

$$B_c = A' + (RR^* + TT^* + SS^*/3)\left(\frac{1}{E_g}\right) + (TT^*/2 + 2SS^*/3)\times\left(\frac{1}{E_g + \Delta}\right),$$

and

$$\Omega_c = \frac{1}{\sqrt{3}}(S^*T + RT^*)\left(\frac{1}{E_g} - \frac{1}{E_g + \Delta}\right).$$

By solving the 2×2 conduction Hamiltonian matrix, the band energy E_c is obtained as

$$E_c = \frac{A_c + B_c}{2} \pm \frac{1}{2}\sqrt{(A_c - B_c)^2 + 4\Omega_c\Omega_c^*}. \tag{5a}$$

Therefore, the spin-splitting energy in the conduction band can be written as

$$\Delta E_c = \frac{2}{3}\sqrt{(SS^* - RR^*)^2 + 3|S^*T + RT^*|^2}\left(\frac{1}{E_g} - \frac{1}{E_g + \Delta}\right). \tag{5b}$$

Similarly, the resulting 2×2 spin-orbit split-off Hamiltonian matrix in the $[hkl]$ orientation can be expressed as

$$H_{2\times 2}^{(so)} = \begin{bmatrix} A_{so} & \Omega_{so} \\ \Omega_{so}^* & B_{so} \end{bmatrix} = \begin{bmatrix} \frac{A_{so} + B_{so}}{2} & 0 \\ 0 & \frac{A_{so} + B_{so}}{2} \end{bmatrix} + \begin{bmatrix} \frac{A_{so} - B_{so}}{2} & \Omega_{so} \\ \Omega_{so}^* & -\frac{A_{so} - B_{so}}{2} \end{bmatrix}, \tag{6}$$

where

$$A_{so} = (P - \Delta) - (QQ + CC^* + DD^*)\left(\frac{2}{\Delta}\right) - (TT^*/2 + 2SS^*/3)\left(\frac{1}{E_g + \Delta}\right),$$

$$B_{so} = (P - \Delta) - (QQ + CC^* + DD^*)\left(\frac{2}{\Delta}\right) - (TT^*/2 + 2RR^*/3)\left(\frac{1}{E_g + \Delta}\right),$$

and

$$\Omega_{so} = -\frac{1}{\sqrt{3}}(S^*T + RT^*)\left(\frac{1}{E_g + \Delta}\right).$$

By solving the 2×2 spin-orbit split-off Hamiltonian matrix, the band energy E_{so} is obtained as

$$E_{so} = \frac{A_{so} + B_{so}}{2} \pm \frac{1}{2}\sqrt{(A_{so} - B_{so})^2 + 4\Omega_{so}\Omega_{so}^*}. \tag{7a}$$

Therefore, the spin-splitting energy in the spin-orbit split-off band can be written as

$$\Delta E_{so} = \frac{2}{3}\sqrt{(SS^* - RR^*)^2 + 3|S^*T + RT^*|^2}\left(\frac{1}{E_g + \Delta}\right). \tag{7b}$$

Under the infinite spin-orbit split-off energy (Δ) approximation, the 6×6 Hamiltonian matrix can be obtained by truncating the spin-orbit split-off band. As in the case of the 8×8 Hamiltonian matrix above, the block diagonal technique can then be applied to the 6×6 Hamiltonian matrix to decouple the conduction band and the hole bands. The resulting 4×4 hole Hamiltonian matrix in the $[hkl]$ orientation has the form

$$H_{4\times4}^{(h)}=\begin{bmatrix}(P+Q)-\frac{SS^*}{E_g} & D-\frac{S^*T}{E_g} & C-\frac{RS^*}{\sqrt{3}E_g} & 0\\ D^*-\frac{ST^*}{E_g} & (P-Q)-\frac{TT^*}{E_g}-\frac{SS^*}{3E_g} & -(RT^*+S^*T)\left(\frac{1}{\sqrt{3}E_g}\right) & C-\frac{RS^*}{\sqrt{3}E_g}\\ C^*-\frac{R^*S}{\sqrt{3}E_g} & -(R^*T+ST^*)\left(\frac{1}{\sqrt{3}E_g}\right) & (P-Q)-\frac{TT^*}{E_g}-\frac{RR^*}{3E_g} & -D-\frac{RT^*}{E_g}\\ 0 & C^*-\frac{R^*S}{\sqrt{3}E_g} & -D^*-\frac{R^*T}{E_g} & (P+Q)-\frac{RR^*}{E_g}\end{bmatrix}. \tag{8}$$

Solving Eq. (8) gives both the heavy (light) hole band energies E_{hh} (E_{lh}) and their corresponding spin-splitting energies ΔE_{hh} (ΔE_{lh}).

Note that the bulk inversion asymmetry effect is already included in the conduction-band ($H_{2\times2}^{(c)}$), hole-band ($H_{4\times4}^{(h)}$), and spin-orbit split-off band ($H_{2\times2}^{(\mathrm{so})}$) matrices.

III. RESULTS AND DISCUSSION

A. [001]-oriented block diagonal Hamiltonian matrices for conduction, hole, and spin-orbit split-off bands

Equation (4) shows the 2×2 Hamiltonian matrix of the conduction band ($H_{2\times2}^{(c)}$) obtained by applying the block diagonal technique to the 8×8 $\boldsymbol{k}\cdot\boldsymbol{p}$ Hamiltonian. By omitting the k^4 terms, Eq. (4) becomes[18–21]

$$H_{2\times2}^{(c)}=H_0^{(c)}+H_{k^3}^{(c)}, \tag{9}$$

where

$$H_0^{(c)}=\begin{bmatrix}E_c+\frac{\hbar^2k^2}{2m_c^*} & 0\\ 0 & E_c+\frac{\hbar^2k^2}{2m_c^*}\end{bmatrix}, \tag{10a}$$

$$H_{k^3}^{(c)}=\gamma_c\{\sigma_xk_x(k_y^2-k_z^2)+\sigma_yk_y(k_z^2-k_x^2)+\sigma_zk_z(k_x^2-k_y^2)\}, \tag{10b}$$

$$\frac{1}{m_c^*}=\frac{1}{m_c}+2\left(\frac{P_0^2}{\hbar^2}\right)\left[\frac{2}{3E_g}+\frac{1}{3(E_g+\Delta)}\right],$$

$$\gamma_c=\frac{2}{3}P_0B_0\left(\frac{1}{E_g}-\frac{1}{E_g+\Delta}\right),$$

$$\sigma_x=\begin{bmatrix}0 & 1\\ 1 & 0\end{bmatrix},$$

$$\sigma_y=\begin{bmatrix}0 & -i\\ i & 0\end{bmatrix},$$

and

$$\sigma_z=\begin{bmatrix}1 & 0\\ 0 & -1\end{bmatrix}.$$

In the expressions above, σ_x, σ_y, and σ_z denote the components of the Pauli spin matrices and γ_c denotes the spin-splitting parameter of the conduction band.[21]

According to Eq. (6), the 2×2 Hamiltonian matrix of the spin-orbit split-off band ($H_{2\times2}^{(\mathrm{so})}$) can be written (when omitting the k^4 terms) as[21]

$$H_{2\times2}^{(\mathrm{so})}=H_0^{(\mathrm{so})}+H_{k^3}^{(\mathrm{so})}, \tag{11}$$

where

$$H_0^{(\mathrm{so})}=\begin{bmatrix}(P-\Delta)-\frac{1}{3}P_0^2k^2\left(\frac{1}{E_g+\Delta}\right) & 0\\ 0 & (P-\Delta)-\frac{1}{3}P_0^2k^2\left(\frac{1}{E_g+\Delta}\right)\end{bmatrix} \tag{12a}$$

and

$$H_{k^3}^{(\mathrm{so})}=-\gamma_{\mathrm{so}}\{\sigma_xk_x(k_y^2-k_z^2)+\sigma_yk_y(k_z^2-k_x^2)+\sigma_zk_z(k_x^2-k_y^2)\}, \tag{12b}$$

in which the spin-splitting parameter of the spin-orbit split-off band has the form

$$\gamma_{\mathrm{so}}=\frac{2}{3}P_0B_0\left(\frac{1}{E_g+\Delta}\right).$$

According to Eq. (8), the 4×4 Hamiltonian matrix of the heavy- and light-hole bands ($H_{4\times4}^{(h)}$) can be written (when omitting the k^4 terms) as[21]

$$H_{4\times4}^{(h)} = H_0^{(h)} + H_{k^3}^{(h)}, \tag{13}$$

where

$$H_0^{(h)} = \begin{bmatrix} P'+Q' & D' & C' & 0 \\ D'^* & P'-Q' & 0 & C' \\ C'^* & 0 & P'-Q' & -D' \\ 0 & C'^* & -D'^* & P'+Q' \end{bmatrix}, \tag{14a}$$

with

$$P' = P - P_0^2(k_x^2+k_y^2+k_z^2)/3E_g,$$

$$Q' = Q - P_0^2(k_x^2+k_y^2-2k_z^2)/6E_g,$$

$$D' = D + P_0^2(k_x - ik_y)k_z/(\sqrt{3}E_g),$$

$$C' = C + P_0^2(k_x - ik_y)^2/(2\sqrt{3}E_g);$$

and

$$H_{k^3}^{(h)} = -\gamma_h\{J_x k_x(k_y^2-k_z^2) + J_y k_y(k_z^2-k_x^2) + J_z k_z(k_x^2-k_y^2)\}, \tag{14b}$$

in which

$$J_x = \begin{bmatrix} 0 & \sqrt{3}/2 & 0 & 0 \\ \sqrt{3}/2 & 0 & 1 & 0 \\ 0 & 1 & 0 & \sqrt{3}/2 \\ 0 & 0 & \sqrt{3}/2 & 0 \end{bmatrix},$$

$$J_y = \begin{bmatrix} 0 & -i\sqrt{3}/2 & 0 & 0 \\ i\sqrt{3}/2 & 0 & -i & 0 \\ 0 & i & 0 & -i\sqrt{3}/2 \\ 0 & 0 & i\sqrt{3}/2 & 0 \end{bmatrix},$$

$$J_z = \begin{bmatrix} 3/2 & 0 & 0 & 0 \\ 0 & 1/2 & 0 & 0 \\ 0 & 0 & 1/2 & 0 \\ 0 & 0 & 0 & 3/2 \end{bmatrix},$$

$$\gamma_h = \frac{2}{3}P_0 B_0\left(\frac{1}{E_g}\right).$$

In the expressions above, J_x, J_y, and J_z denote the components of the angular momentum operator on the $J=3/2$ hole band states and γ_h is the spin-splitting parameter of the hole band.[21]

B. Spin-splitting expressions for zincblende bulk

When $k_{x'}=k_{y'}=0$ and $k_{z'}=k$, the Hamiltonian matrix elements have the forms

$$S = R^* = \tfrac{1}{\sqrt{2}}B_0 k^2[-(O_{12}O_{23}O_{33} + O_{22}O_{13}O_{33} + O_{32}O_{13}O_{23}) + i(O_{11}O_{23}O_{33} + O_{21}O_{13}O_{33} + O_{31}O_{13}O_{23})], \tag{15a}$$

$$T = \tfrac{\sqrt{2}}{\sqrt{3}}P_0 k - i\tfrac{\sqrt{2}}{\sqrt{3}}B_0 k^2(O_{13}O_{23}O_{33} + O_{23}O_{13}O_{33} + O_{33}O_{13}O_{23}), \tag{15b}$$

and

$$SS^* = RR^*. \tag{15c}$$

From Eqs. (5b) and (15a)–(15c), the conduction band spin-splitting energy of zincblende bulk in any arbitrary **k** direction can be expressed as

$$\Delta E_c = \frac{4\sqrt{2}}{3}P_0 k\sqrt{SS^*}\left(\frac{1}{E_g} - \frac{1}{E_g+\Delta}\right). \tag{16}$$

1. Spin-splitting along the arbitrary k direction

If the electron wave vector **k** is oriented along the direction (k,θ,ϕ) in spherical coordinates, then $\mathbf{k} = k\sin\theta\cos\phi\hat{x} + k\sin\theta\sin\phi\hat{y} + k\cos\theta\hat{z}$ and the rotation matrix required for coordinate transformation has the form[15]

$$O_T = \begin{bmatrix} \cos\theta\cos\phi & -\sin\phi & \sin\theta\cos\phi \\ \cos\theta\sin\phi & \cos\phi & \sin\theta\sin\phi \\ -\sin\theta & 0 & \cos\theta \end{bmatrix}, \tag{17}$$

where $\theta(=\cos^{-1}k_z/k)$ and $\phi(=\cos^{-1}k_x/\sqrt{k_x^2+k_y^2})$ represent the polar angle and the azimuthal angle, respectively, of the direction of **k** relative to the (x,y,z) lattice coordinate system.

From Eqs. (15a)–(15c), (16), and (17), the conduction band spin-splitting energy of zincblende bulk in any arbitrary **k** direction can be expressed as[18–21]

$$\Delta E_c = 2\gamma_c[k_x^2(k_y^2-k_z^2)^2 + k_y^2(k_z^2-k_x^2)^2 + k_z^2(k_x^2-k_y^2)^2]^{1/2} = 2\gamma_c k\{|\vec{q}\times\hat{k}|^2\}^{1/2}, \tag{18}$$

where

$$\vec{q} = k_y k_z\hat{x} + k_z k_x\hat{y} + k_x k_y\hat{z} \quad \text{and} \quad \hat{k} = \frac{k_x}{k}\hat{x} + \frac{k_y}{k}\hat{y} + \frac{k_z}{k}\hat{z}.$$

The value of the spin-splitting effect is determined by the cubic-in-k term. The spin-splitting energy attains its maximum value when **k** is oriented along the [110] direction and has a value of zero when **k** is aligned along either the [001] or the [111] direction.

2. In-plane spin-splitting expressions for [hkl]-grown epitaxial layers

If the direction of the electron wave vector **k** coincides with the growth direction of the epitaxial layer on the $[hkl]$-oriented substrate, the rotation matrix required for coordinate transformation has the form

$$O_T = \begin{bmatrix} -\sin\beta\cos\gamma & -\sin\alpha\cos\beta\cos\gamma - \cos\alpha\sin\gamma & \cos\alpha\cos\beta\cos\gamma - \sin\alpha\sin\gamma \\ -\sin\beta\sin\gamma & -\sin\alpha\cos\beta\sin\gamma + \cos\alpha\cos\gamma & \cos\alpha\cos\beta\sin\gamma + \sin\alpha\cos\gamma \\ -\cos\beta & \sin\alpha\sin\beta & -\cos\alpha\sin\beta \end{bmatrix}, \tag{19}$$

where $\beta(=\tan^{-1}\sqrt{h^2+k^2}/l)$ and $\gamma(=\tan^{-1}k/h)$ represent the polar and azimuthal angles, respectively, of the growth direction relative to the (x,y,z) lattice coordinate system. The rotation is specified by its corresponding angles α, β, and γ. The growth direction is determined by specifying the rotation of β and γ, while the in-plane direction is governed by α [i.e., $\alpha=\tan^{-1}(k_{y'}/k_{x'})$].

From Eqs. (15a)–(15c), (16), and (19), the in-plane spin-splitting energy of zincblende semiconductor layers grown on [001]-, [111]-, and [110]-oriented substrates can be expressed as

$$\Delta E_c(k_\parallel)_{[001]} = \gamma_c k_\parallel^3 |\sin 2\alpha|, \tag{20a}$$

$$\Delta E_c(k_\parallel)_{[111]} = \frac{\gamma_c}{\sqrt{3}} k_\parallel^3 \{2(3\cos^2\alpha - \sin^2\alpha)^2 \sin^2\alpha + 1\}^{1/2}, \tag{20b}$$

and

$$\Delta E_c(k_\parallel)_{[110]} = \gamma_c k_\parallel^3 |\sin\alpha(2\cos^2\alpha - \sin^2\alpha)|, \tag{20c}$$

respectively, where $k_\parallel$ represents the magnitude of the in-plane wave vector.

It is observed that Eqs. (18) and (20a)–(20c) contain cubic-in-k terms but have no even-in-k terms due to the time reversal symmetry properties of zincblende semiconductors. By directly solving Eq. (18) by taking GaAs zincblende bulk as an example, the spin-splitting energy of the conduction band can be obtained for any arbitrary $\mathbf{k}=[0.03(2\pi/a)]$ direction, as shown in Fig. 1. It can be seen that the high symmetry of the bulk material results in zero spin-splitting energies along the $\langle 001\rangle$ and $\langle 111\rangle$ directions. The in-plane spin-splitting patterns for [001]-, [111]-, and [110]-grown GaAs epitaxial layers can be obtained by solving Eqs. (20a)–(20c), respectively, by using the experimental value of $\gamma_c=20.9$ eV Å^3 for GaAs.[22] Note that these patterns are not presented here because they are virtually identical to those of both GaAs bulk and GaAs QWs with wide well widths and large in-plane wave vectors, as shown in Figs. 2(a)–2(c).

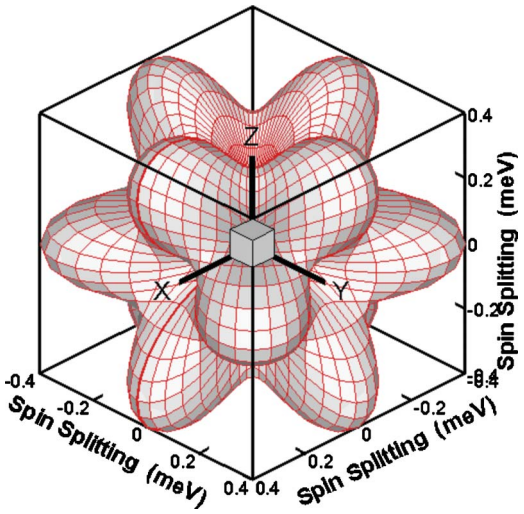

FIG. 1. (Color online) Spin splitting of the GaAs bulk conduction band as a function of the direction of wave vector **k**. Note that **k** has a constant magnitude of $0.03(2\pi/a)$.

C. In-plane spin-splitting expressions for [001]-, [111]-, and [110]-grown QWs

In Eq. (9), the matrix $H_0^{(c)}$ is the same for any arbitrary-growth-direction substrate, and $H_{k^3}^{(c)}$ [see Eq. (4)] can be expressed as[18–21]

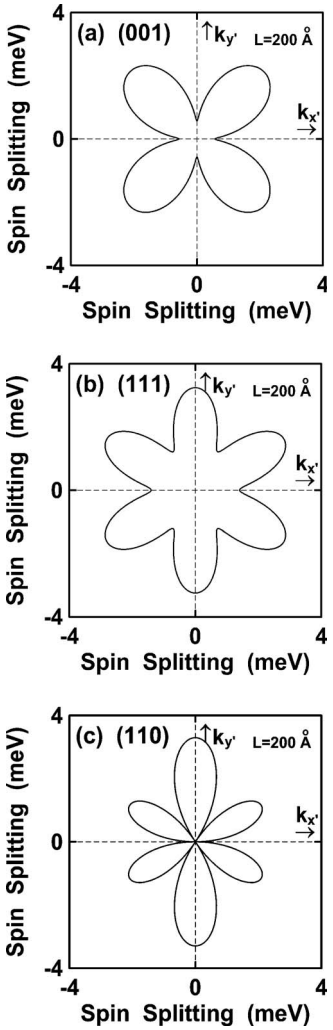

FIG. 2. Spin splitting of the first conduction subband of (a) [001]-, (b) [111]-, and (c) [110]-grown GaAs QWs with a well width of $L=200$ Å as a function of the direction of **k**. Note that **k** has a constant magnitude of $0.05(2\pi/a)$ and an infinite-barrier-height assumption is imposed.

$$H_{k^3}^{(c)} = \gamma_c \begin{bmatrix} k_z(k_x^2 - k_y^2) & k_x(k_y^2 - k_z^2) - ik_y(k_z^2 - k_x^2) \\ k_x(k_y^2 - k_z^2) + ik_y(k_z^2 - k_x^2) & -k_z(k_x^2 - k_y^2) \end{bmatrix} \tag{21a}$$

for [001]-grown QWs with $x \| [100]$, $y \| [010]$, and $z \| [001]$, or as

$$H_{k^3}^{(c)} = \frac{\gamma_c}{2\sqrt{3}} \begin{bmatrix} \sqrt{2}k_{y'}(3k_{x'}^2 - k_{y'}^2) & \left\{ \begin{matrix} [-k_{y'}(k_{x'}^2 + k_{y'}^2) + k_{y'}k_{z'}(4k_{z'} - 2\sqrt{2}k_{x'})] \\ +i[-k_{x'}(k_{x'}^2 + k_{y'}^2) + \sqrt{2}k_{z'}(k_{x'}^2 - k_{y'}^2) + 4k_{x'}k_{z'}^2] \end{matrix} \right\} \\ \left\{ \begin{matrix} [-k_{y'}(k_{x'}^2 + k_{y'}^2) + k_{y'}k_{z'}(4k_{z'} - 2\sqrt{2}k_{x'})] \\ -i[-k_{x'}(k_{x'}^2 + k_{y'}^2) + \sqrt{2}k_{z'}(k_{x'}^2 - k_{y'}^2) + 4k_{x'}k_{z'}^2] \end{matrix} \right\} & -\sqrt{2}k_{y'}(3k_{x'}^2 - k_{y'}^2) \end{bmatrix} \tag{21b}$$

for [111]-grown QWs with $x' \| [11\bar{2}]$, $y' \| [\bar{1}10]$, and $z' \| [111]$, or finally as

$$H_{k^3}^{(c)} = \gamma_c \begin{bmatrix} k_{y'}\left(k_{x'}^2 - \frac{1}{2}k_{y'}^2\right) + \frac{1}{2}k_{y'}k_{z'}^2 & -2k_{x'}k_{y'}k_{z'} + ik_{z'}\left(-k_{x'}^2 - \frac{1}{2}k_{y'}^2 + \frac{1}{2}k_{z'}^2\right) \\ -2k_{x'}k_{y'}k_{z'} - ik_{z'}\left(-k_{x'}^2 - \frac{1}{2}k_{y'}^2 + \frac{1}{2}k_{z'}^2\right) & -k_{y'}\left(k_{x'}^2 - \frac{1}{2}k_{y'}^2\right) - \frac{1}{2}k_{y'}k_{z'}^2 \end{bmatrix} \tag{21c}$$

for [110]-grown QWs with $x' \| [00\bar{1}]$, $y' \| [\bar{1}10]$, and $z' \| [110]$. In the expressions above, the rotation matrix given in Eq. (17) is applied to the [111]- and [110]-oriented calculations on the rotation of the wave vectors and the linear combination coefficients of the basis.

Under the infinite-barrier-height and envelope-function approximations, the QW envelope functions for the conduction band become simple sinusoidal waves. If the $H_{2\times 2}^{(c)} = H_0^{(c)} + H_{k^3}^{(c)}$ matrix is solved by using a first-order perturbation theory (i.e., the k^3 matrix is treated as a perturbation term),[11,18,20] the in-plane spin-splitting energies of [001]-, [111]-, and [110]-grown QWs can be obtained as[18]

$$\Delta E_c(k_\parallel)_{[001]} = \gamma_c \{4k_\parallel^2 \langle k_z^2 \rangle^2 - 4k_\parallel^4 \sin^2 2\alpha \langle k_z^2 \rangle + k_\parallel^6 \sin^2 2\alpha\}^{1/2}, \tag{22a}$$

$$\Delta E_c(k_\parallel)_{[111]} = \gamma_c \left\{ \frac{16}{3}k_\parallel^2 \langle k_{z'}^2 \rangle^2 - \frac{8}{3}k_\parallel^4 \langle k_{z'}^2 \rangle + \frac{1}{3}k_\parallel^6 [2(3\cos^2\alpha - \sin^2\alpha)^2 \sin^2\alpha + 1] \right\}^{1/2}, \tag{22b}$$

and

$$\Delta E_c(k_\parallel)_{[110]} = \gamma_c \{k_\parallel^2 \sin^2\alpha \langle k_{z'}^2 \rangle^2 + 2k_\parallel^4 \sin^2\alpha (2\cos^2\alpha - \sin^2\alpha) \langle k_{z'}^2 \rangle + k_\parallel^6 \sin^2\alpha (2\cos^2\alpha - \sin^2\alpha)^2\}^{1/2}, \tag{22c}$$

respectively, where $\alpha = \tan^{-1}(k_{x'}/k_{y'})$. In these expressions, $k_{z'}$ is quantized as follows:[20] $\langle k_{z'} \rangle = 0$, $\langle k_{z'}^3 \rangle = 0$, and $\langle k_{z'}^2 \rangle = \int \phi(z')^* (-i\partial/\partial z')^2 \phi(z') dz' = (\pi/L)^2$, where L is the well width and $\phi(z')$ is the electron envelope function in the well for $H_0^{(c)}$. It is observed that these expressions contain both linear-in-k and cubic-in-k terms for $k_\parallel$. In the following calculations, it is shown that the spin-splitting energies linearly (cubically) depend on in-plane wave vectors $k_\parallel$ relative to the small (large) quantized $k_{z'}$ vector.

Figures 2(a)–2(c) show the spin-splitting energies of the first conduction subband of [001]-, [111]-, and [110]-grown GaAs QWs, respectively, as a function of the direction of $\mathbf{k}_\parallel$. Note that the well width is $L = 200$ Å in every case and $k_\parallel$ has a magnitude of $0.05(2\pi/a)$. When the QW has a wide well width and $k_\parallel$ has a substantial magnitude, the interband mixing effect is strong; thus, Figs. 2(a)–2(c) show evidence of a band warping phenomenon in the conduction subbands. Furthermore, it is evident that the in-plane spin-splitting patterns strongly depend on the growth direction of the QW. Specifically, the in-plane spin-splitting patterns for the [001]-, [111]-, and [110]-grown QWs are strongly anisotropic with fourfold, sixfold, and twofold symmetries, respectively. Importantly, the axes of the in-plane patterns lie along the directions of the tetragonal bonds projected on the layer plane. As a result, the anisotropic spin-splitting phenomenon is strongly affected by the anisotropy of the geometrical arrangement of the tetragonal bonds.

Figures 3(a)–3(c) show the in-plane spin-splitting patterns for QWs of well width $L = 50$ Å that are grown along the [001], [111], and [110] directions, respectively. Note that the magnitude of the wave vector is $k_\parallel = 0.05(2\pi/a)$ in every case. By comparing Figs. 2 and 3, it is seen that the spin-splitting pattern is strongly dependent on the QW width. For the case wherein the QW has a high well width and the wave vector has a substantial magnitude (Fig. 2), the in-plane spin-splitting pattern closely resembles that of the bulk material calculated in Sec. III B 2. Furthermore, in Eqs. (22a)–(22c), the coefficients of the $\langle k_{z'}^2 \rangle^0$ terms, which cubically depend on the wave vector $k_\parallel$, are the same as those in Eqs. (20a)–(20c). However, in the small-well-width QW case

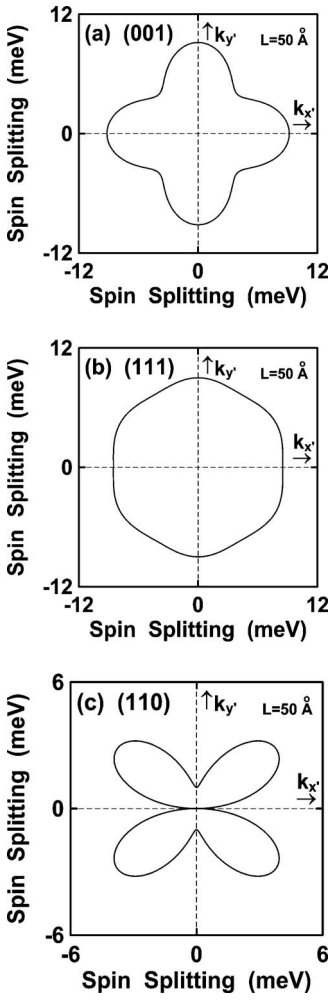

FIG. 3. Spin splitting of the first conduction subband of (a) [001]-, (b) [111]-, and (c) [110]-grown GaAs QWs with a well width of $L=50$ Å as a function of the direction of **k**. Note that **k** has a constant magnitude of $0.05(2\pi/a)$ and an infinite-barrier-height assumption is imposed.

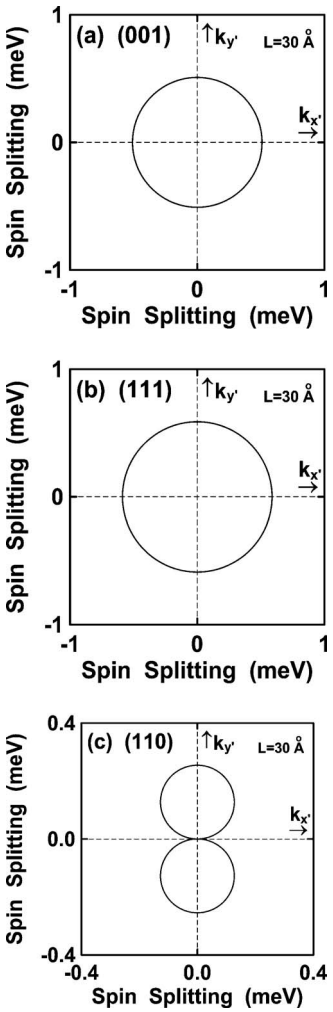

FIG. 4. Spin splitting of the first conduction subband of (a) [001]-, (b) [111]-, and (c) [110]-grown GaAs QWs with a well width of $L=30$ Å as a function of the direction of **k**. Note that **k** has a constant magnitude of $0.001(2\pi/a)$ and an infinite-barrier-height assumption is imposed.

(Fig. 3), the term containing $\langle k_{z'}^2 \rangle^2$ dominates, and thus, the spin-splitting energy linearly depends on the magnitude of $k_{\|}$.

Figures 4(a)–4(c) show the in-plane spin-splitting patterns for QWs with a well width of $L=30$ Å that are grown along the [001], [111], and [110] directions, respectively. Note that $k_{\|}=0.001(2\pi/a)$ in every case. The spin-splitting patterns in Figs. 4(a)–4(c) are notably different from those presented in Figs. 2(a)–2(c) or Figs. 3(a)–3(c). The narrow well width and small magnitude of the wave vector considered in Fig. 4 reduce the extent of the interband mixing effect, and thus, band warping does not take place. As a result, the shape of the in-plane spin-splitting patterns primarily depends on the microscopic symmetry of the QW. Regarding the bulk inversion asymmetry property, the [001]- and [111]-grown QWs exhibit relatively high-symmetry C_{2v} and C_{3v}, respectively, while the [110]-grown QW shows relatively low-symmetry C_{1h}. The lower symmetry of the tetragonal bond arrangement results in an additional mixing effect, which leads to the in-plane anisotropy of spin splitting. Thus, as shown in Fig. 4(c), a highly anisotropic spin-splitting pattern (resembling a dumbbell) is produced. Therefore, in QWs with a narrow well width and a low magnitude of $k_{\|}$, the geometrical shape of the in-plane spin-splitting patterns strongly depends on the microscopic symmetry of the QW.

IV. CONCLUSIONS

This paper has applied the block diagonal technique to the $[hkl]$-oriented 8×8 $\boldsymbol{k}\cdot\boldsymbol{p}$ Hamiltonian matrix for zincblende semiconductors to obtain the corresponding 2×2 conduction band, 4×4 hole band, and 2×2 spin-orbit split-off band matrices. Importantly, the block diagonal matrices incorporate not only the interband coupling effect but also the bulk inversion asymmetry effect. The calculation results have shown that the bulk inversion asymmetry in the block diagonal matrix representation is consistent with the results from the viewpoint of symmetry. By solving the block diagonal matrices, analytical expressions have been obtained for the conduction band spin-splitting energies of both zincblende bulk and quantum wells grown on [001]-, [111]-, and [110]-oriented substrates.

ACKNOWLEDGMENTS

The current authors gratefully acknowledge the financial support provided to this study by the National Science Council of Taiwan, R.O.C., under Grant No. NSC-96-2221-E-269-024.

[1]I. Lo, W. T. Wang, M. H. Gau, S. F. Tsay, and J. C. Chiang, Phys. Rev. B **72**, 245329 (2005).
[2]I. Lo, W. T. Wang, M. H. Gau, S. F. Tsay, and J. C. Chiang, Appl. Phys. Lett. **88**, 082108 (2006).
[3]D. Z.-Y. Ting and X. Cartoixà, Phys. Rev. B **68**, 235320 (2003).
[4]P. Pfeffer and W. Zawadzki, Phys. Rev. B **72**, 035325 (2005).
[5]L. Jiang and M. W. Wu, Phys. Rev. B **72**, 033311 (2005).
[6]G. Bastard, Phys. Rev. B **46**, 4253 (1992).
[7]H. L. Störmer, Z. Schlesinger, A. Chang, D. C. Tsui, A. C. Gossard, and W. Wiegmann, Phys. Rev. Lett. **51**, 126 (1983).
[8]J. P. Eisenstein, H. L. Störmer, U. Narayanaumurti, A. C. Gossard, and W. Wiegmann, Phys. Rev. Lett. **53**, 2579 (1984).
[9]G. Dresselhaus, Phys. Rev. **100**, 580 (1955).
[10]Y. A. Bychkov and E. I. Rashba, J. Phys. C **17**, 6039 (1984).
[11]E. O. Kane, in *Semiconductors and Semimetals*, edited by R. K. Willardson and A. C. Beer (Academic, New York, 1966), Vol. 1, pp. 75–100.
[12]M. Cardona, N. E. Christensen, and G. Fasol, Phys. Rev. Lett. **56**, 2831 (1986).
[13]S. F. Alvarado, H. Riechert, and N. E. Christensen, Phys. Rev. Lett. **55**, 2716 (1985).
[14]D. Stein, K. V. Klitzing, and G. Weiman, Phys. Rev. Lett. **51**, 130 (1983).
[15]C. N. Chen, Phys. Rev. B **72**, 085305 (2005).
[16]C. N. Chen, J. Appl. Phys. **96**, 7374 (2004).
[17]Y. C. Chang, Phys. Rev. B **37**, 8215 (1988).
[18]R. Eppenga and M. F. H. Schuurmans, Phys. Rev. B **37**, 10923 (1988).
[19]B. Das and S. Datta, Phys. Rev. B **41**, 8278 (1990).
[20]T. Hassenkam, S. Pedersen, K. Baklanov, A. Kristensen, C. B. Sorensen, P. E. Lindelof, F. G. Pikus, and G. E. Pikus, Phys. Rev. B **55**, 9298 (1997).
[21]E. L. Ivchenko and G. E. Pikus, *Superlattices and Other Heterostructures* (Springer-Verlag, Berlin, 1995), Chap. 3.
[22]T. E. Ostromek, Phys. Rev. B **54**, 14467 (1996).